npj | climate and atmospheric science

www.nature.com/npjclimatsci

BRIEF COMMUNICATION OPEN

Check for updates

The ratio of mesoscale convective system precipitation to total precipitation increases in future climate change scenarios

Alex M. Haberlie[1]✉, Walker S. Ashley[1], Victor A. Gensini[1] and Allison C. Michaelis[1]

Mesoscale convective systems (MCSs) are a substantial source of precipitation in the eastern U.S. and may be sensitive to regional climatic change. We use a suite of convection-permitting climate simulations to examine possible changes in MCS precipitation. Specifically, annual and regional totals of MCS and non-MCS precipitation generated during a retrospective simulation are compared to end-of-21st-century simulations based on intermediate and extreme climate change scenarios. Both scenarios produce more MCS precipitation and less non-MCS precipitation, thus significantly increasing the proportion of precipitation associated with MCSs across the U.S.

npj Climate and Atmospheric Science (2023)6:150 ; https://doi.org/10.1038/s41612-023-00481-5

INTRODUCTION

Mesoscale convective systems (MCSs) and their precipitation are important to regional hydroclimates and, thus, numerous aspects of society[1]. Concerningly, MCS precipitation may be changing[2,3], and at a rate differing from other types of precipitation events[4] (non-MCS precipitation). This is important because the character MCS and non-MCS precipitation (e.g., rate, duration, areal coverage, etc.) are fundamentally different[5–7] and produce contrasting hydrological responses[8] and societal impacts[9,10]. However, few studies have examined future changes in MCS precipitation[11], and none have examined how MCS precipitation may change relative to non-MCS precipitation due to the difficulties associated with running convection-permitting regional climate models (CP-RCMs[12,13]). Although CP-RCMs are necessary for properly simulating meso-gamma processes associated with deep, moist convection (including MCSs[14]), few CP-RCM climate change simulations with sufficiently long study periods (e.g., ≥ 10 years) and domains encompassing the conterminous United States (CONUS) exist[15–19]. CP-RCMs are capable of decomposing MCS and non-MCS precipitation, and examining how these two categories of precipitation respond to climate change scenarios will improve our understanding of regional climate change in the central and eastern CONUS[1,20]. Using a suite of simulations driven by a CP-RCM[19], we examine how MCS and non-MCS precipitation may change relative to one another in two potential climate change realizations.

PRECIPITATION IN A RETROSPECTIVE AND TWO END-OF-CENTURY SIMULATIONS

We assess trends in MCS, non-MCS precipitation, and total (ALL) precipitation using output from a CP-RCM for a retrospective simulation (*HIST*; 1990–2005) and two end-of-21st-century (*FUTR 4.5* and *FUTR 8.5*; 2085–2100) simulations. The spatial pattern of MCS precipitation in HIST (Fig. 1b) is similar to observations[21]. MCS precipitation accumulation in HIST maximizes over Louisiana and decreases in step with distance from the Gulf of Mexico, while non-MCS precipitation maximizes over parts of the Northeast (Fig. 1c). For the eastern CONUS (ECONUS; Fig. 1a.i–v), the spatial pattern of ALL precipitation is more correlated with non-MCS precipitation than it is with MCS precipitation ($r_{non\_mcs} = 0.75$; $r_{mcs} = 0.66$; $p < 0.05$). The difference in spatial correlation between ALL precipitation and MCS and non-MCS precipitation is smallest for the Southern Plains ($r_{non\_mcs} = 0.97$; $r_{mcs} = 0.99$; $p < 0.05$) and largest for the Northeast ($r_{non\_mcs} = 0.91$; $r_{mcs} = 0.40$; $p < 0.05$). Previous work examining MCS and non-MCS precipitation in observational datasets reported similar findings[4].

Two regimes of ALL precipitation trends exist in both FUTR 4.5 and FUTR 8.5 across the ECONUS, with increasingly dry years in the central and southern Great Plains, and increasingly wet years in the Midwest, Northeast, and Mid-South (Fig. 1d, g). This pattern is also evident in MCS precipitation trends (Fig. 1e, h), except there are more grids with significant increases. Conversely, non-MCS precipitation decreases in both FUTR 4.5 and FUTR 8.5 for most locations in the ECONUS (Fig. 1f, i). Consequently, the ratio of MCS precipitation to ALL precipitation increases significantly over most of the ECONUS for annual (Supplementary Fig. 1) and seasonal periods (Supplementary Figs. 2, 3, 4, and 5) in FUTR 8.5, and over smaller portions of the ECONUS in FUTR 4.5. The distribution of regional means of annual precipitation in HIST, FUTR 4.5, and FUTR 8.5 for ALL events, MCS events, and non-MCS events further illustrates these trends (Fig. 2). Generally, annual totals of ALL precipitation stay the same (Fig. 2a), annual MCS precipitation increases (Fig. 2b), annual non-MCS precipitation decreases (Fig. 2c). As a result, the ratio of MCS to ALL precipitation significantly increases for all regions in FUTR 8.5, and all but the Northern Plains in FUTR 4.5 (Fig. 2b). Only one region, the Southern Plains, experiences significant decreases in ALL precipitation, whereas multiple regions experience significant increases in MCS precipitation (ECONUS, Midwest, Southeast, and Northeast), significant decreases in non-MCS precipitation (ECONUS, Southern Plains, Midwest, and Southeast), or both (ECONUS, Midwest, Southeast, Northeast). For the Southern Plains, a significant decrease in non-MCS precipitation is the main driver of decreases in ALL precipitation in both climate change scenarios. In contrast, significant decreases in non-MCS precipitation in FUTR 8.5 for the Midwest and Southeast are offset by significant increases in MCS precipitation, resulting in no significant differences in ALL precipitation. The Northeast is the only region

[1]Department of Earth, Atmosphere, and Environment, Northern Illinois University, DeKalb, IL, USA. ✉email: ahaberlie1@niu.edu

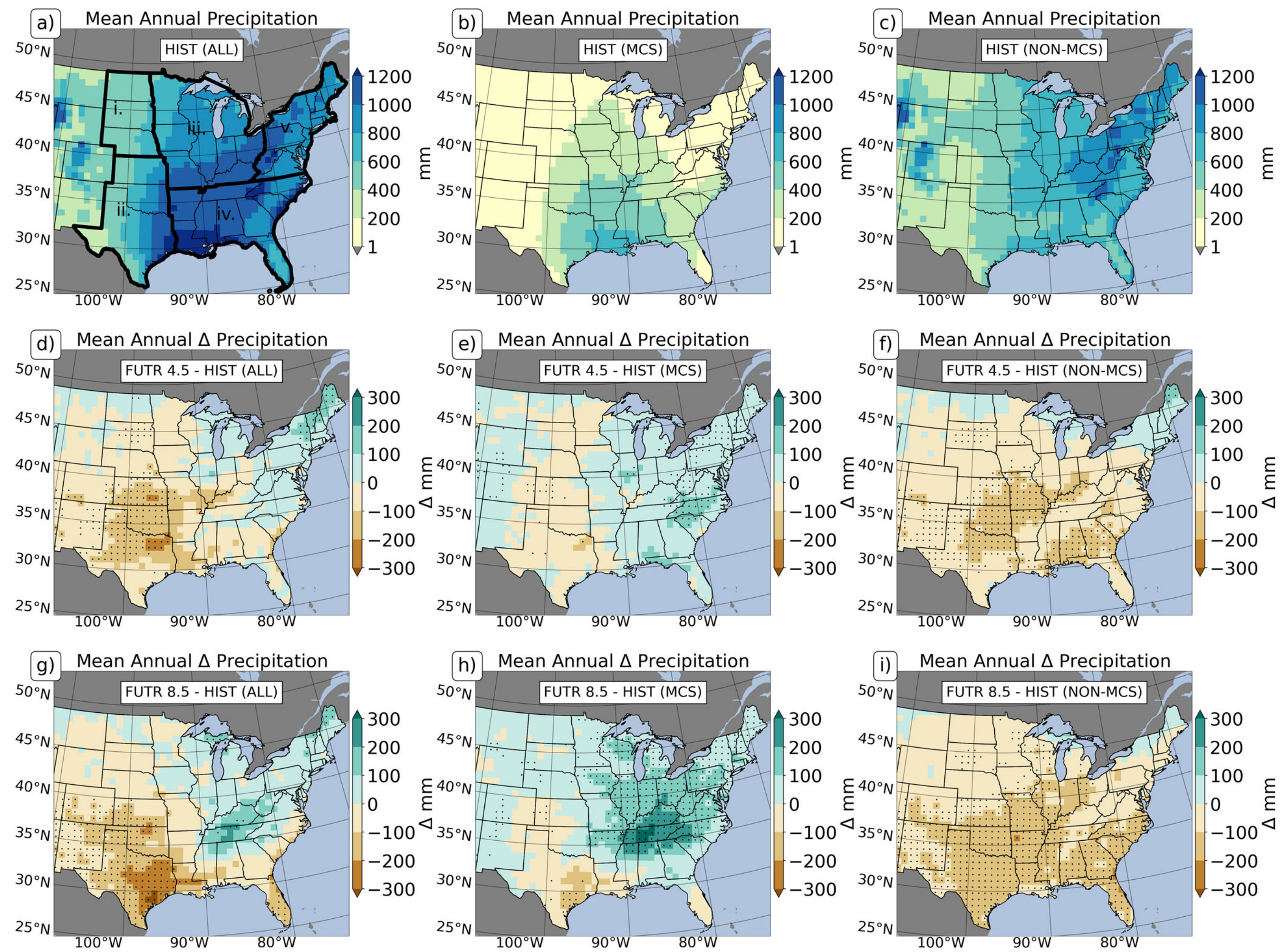

Fig. 1 Changes in Mean Annual MCS and NON-MCS Precipitation. Mean annual precipitation stratified by event type for (**a**–**c**) HIST and the change in mean annual precipitation relative to HIST for (**d**–**f**) FUTR 4.5 and (**g**–**i**) FUTR 8.5. Event types include (**a**, **d**, **g**) ALL events, (**b**, **e**, **h**) MCS events, and (**c**, **f**, **i**) NON-MCS events (i.e., Precipitation from ALL events - Precipitation from MCS events). Significant differences relative to HIST are noted in (**d**–**i**) using the Mann–Whitney U test ($p < 0.05$). The subregions in (**a**) are the (i) Northern Plains, (ii) Southern Plains, (iii) Midwest, (iv) Southeast, and (v) Northeast. The eastern CONUS (ECONUS) is defined as the combination of regions i–v.

to experience significant increases in MCS precipitation in both FUTR 4.5 and FUTR 8.5.

DISCUSSION

Since MCSs are often associated with high precipitation rates that can be extreme and distributed over large areas for extended periods[5–7], "replacing" non-MCS precipitation with MCS precipitation may result in fundamentally different hydrologic responses[8]. Thus, even for locations without significant changes in ALL precipitation, the "character" of precipitation may change[22]. Differing trends in MCSs and non-MCS precipitation may be related to projected increases in instability and convective inhibition[23–26] and the resulting suppression of weak convection[1]. MCSs may also have an advantage over non-MCS events in the future due to possible increases in updraft size[11] and stronger cold pools[27]. Future work will use CP-RCM output from multiple climate change scenarios to specifically examine the duration, intensity, and recurrence of future precipitation events, pertinent environmental changes, and potential influences on hydrologic responses.

METHODS

Regional climate modeling approach

Mesoscale convective system (MCS) activity is simulated for a retrospective period (*HIST*; 1990–2005), and two end-of-21st-century climate change scenarios (*FUTR 4.5* and *FUTR 8.5*; 2085–2100). We use RCP 4.5 and RCP 8.5 from the Community Earth System Model (bias-corrected CESM[28,29]) and the Weather Research and Forecasting Model (WRF-ARW v.4.1.2) to perform dynamical downscaling to a 3.75 km grid encompassing the CONUS[19]. Variables such as accumulated precipitation and simulated composite reflectivity[30] are saved at 15 min intervals. Precipitation produced by the model is consistent with long-term observations[19], and the frequency of various simulated reflectivity thresholds are consistent with observations[25]. These two variables are commonly used to identify proxies of thunderstorm activity, including MCSs, in CP-RCMs[11,14,23–25,31].

Identifying MCS precipitation

MCSs are identified in simulated composite (column maximum) reflectivity grids as in previous work[31]: (1) MCS slices are extracted from 15 min simulated composite reflectivity (Supplementary Fig. 6); (2) Qualifying MCS slices are tracked using spatial overlap

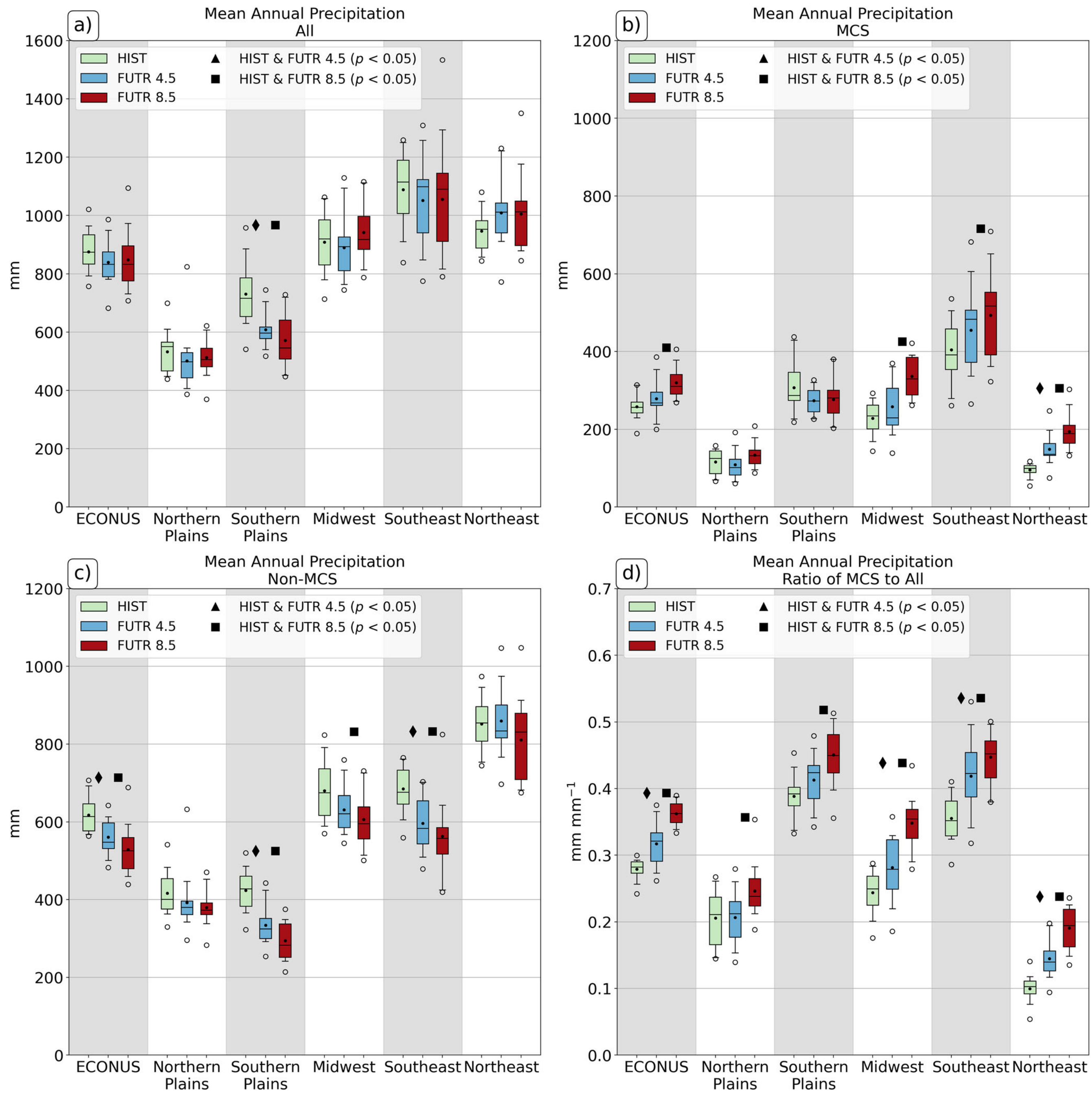

Fig. 2 Regional Variability in Mean Annual MCS and NON-MCS Precipitation. Regional means of mean annual precipitation accumulation (**a**–**c**) and mean annual ratios of MCS to ALL precipitation (**d**) for 15 respective simulation years (HIST, FUTR 4.5, and FUTR 8.5) for the regions denoted in Fig. 1. Boxes represent the interquartile range, dots within the boxes are the means, lines within the boxes are medians, whiskers represent the 5–95th percentile range, and outliers denoted by unfilled circles. Significant differences—determined by a p value < 0.05 using the Mann–Whitney U test—between HIST and FUTR 4.5 (FUTR 8.5) are denoted by black diamonds (squares) above the maximum outliers.

detection, with ties (Supplementary Figs. 7 and 8) broken by matching the most similar overlapping slices[32]; and (3) Only those tracks that last at least 3 h are considered. ALL precipitation is the unfiltered annual or seasonal accumulation. MCS precipitation is filtered by considering only grids that share spatiotemporal pixel coordinates with qualifying MCS tracks. ALL and MCS precipitation are upscaled to a ~ 75 km grid by finding the 20 × 20 grid mean of accumulated annual or seasonal precipitation for each event type. Finally, non-MCS precipitation is the difference between ALL and MCS precipitation. The study area includes only CONUS regions (Fig. 1) with the highest MCS frequencies[21].

Limitations

Each 15-year simulation used one set of model parameters and one GCM due to the computational demands of CP-RCMs[12,13]. Thus, long term (≥10 yr) climatic variability, the impact of various model parameter choices[27,33,34], and the influence of different parent GCMs is under sampled. The modeling approach used for this work[19] did result in incremental improvements in simulating annual and seasonal precipitation over the CONUS relative to recent work[18]. That said, there are still deficiencies that may influence the results discussed in this paper, such as a general warm season dry bias in the ECONUS—specifically, parts of the Southeast CONUS during the summer. Because of these issues, the results presented here should only be interpreted as differences between the retrospective and climate change simulations, and not differences relative to current observations. Future work should leverage emerging computational capabilities to further explore these areas of uncertainty.

DATA AVAILABILITY

The datasets generated during and/or analyzed during the current study are available at https://svrimg.niu.edu/npjcas23/.

CODE AVAILABILITY

The code used for this study is available on GitHub (https://github.com/ahaberlie/MCS_Ratios).

Received: 28 May 2023; Accepted: 14 September 2023;
Published online: 26 September 2023

REFERENCES

1. Schumacher, R. S. & Rasmussen, K. L. The formation, character and changing nature of mesoscale convective systems. *Nat. Rev. Earth Environ.* **1**, 300–314 (2020).
2. Kunkel, K. E. et al. Meteorological causes of the secular variations in observed extreme precipitation events for the conterminous United States. *J. Hydrometeorol.* **13**, 1131–1141 (2012).
3. Feng, Z. et al. More frequent intense and long-lived storms dominate the springtime trend in central US rainfall. *Nat. Commun.* **7**, 13429 (2016).
4. Hu, H., Leung, L. R. & Feng, Z. Observed warm-season characteristics of MCS and non-MCS rainfall and their recent changes in the central United States. *Geophys. Res. Lett.* **47**, e2019GL086783 (2020).
5. Schumacher, R. S. & Johnson, R. H. Characteristics of US extreme rain events during 1999–2003. *Weather Forecast* **21**, 69–85 (2006).
6. Peters, J. M. & Schumacher, R. S. Mechanisms for organization and echo training in a flash-flood-producing mesoscale convective system. *Mon. Weather Rev.* **143**, 1058–1085 (2015).
7. Hu, H., Feng, Z. & Leung, L. R. Linking flood frequency with mesoscale convective systems in the US. *Geophys. Res. Lett.* **48**, e2021GL092546 (2021).
8. Pal, S., Wang, J., Feinstein, J., Yan, E. & Kotamarthi, V. R. Projected changes in extreme streamflow and inland flooding in the mid-21st century over Northeastern United States using ensemble WRF-Hydro simulations. *J. Hydrol. Reg. Stud.* **47**, 101371 (2023).
9. Ashley, S. T. & Ashley, W. S. The storm morphology of deadly flooding events in the United States. *Int. J. Climatol.* **28**, 493–503 (2008).
10. Ashley, W. S., Haberlie, A. M. & Strohm, J. A climatology of quasi-linear convective systems and their hazards in the United States. *Weather Forecast* **34**, 1605–1631 (2019).
11. Prein, A. F. et al. Increased rainfall volume from future convective storms in the US. *Nat. Clim. Change* **7**, 880–884 (2017).
12. Kendon, E. J., Prein, A. F., Senior, C. A. & Stirling, A. Challenges and outlook for convection-permitting climate modelling. *Philos. Trans. R. Soc. A* **379**, 20190547 (2021).
13. Fowler, H. J. et al. Anthropogenic intensification of short-duration rainfall extremes. *Nat. Rev. Earth Environ.* **2**, 107–122 (2021).
14. Prein, A. F. et al. Simulating North American mesoscale convective systems with a convection-permitting climate model. *Clim. Dyn.* **55**, 95–110 (2020).
15. Gensini, V. A. & Mote, T. L. Estimations of hazardous convective weather in the United States using dynamical downscaling. *J. Clim.* **27**, 6581–6598 (2014).
16. Gensini, V. A. & Mote, T. L. Downscaled estimates of late 21st century severe weather from CCSM3. *Clim. Change* **129**, 307–321 (2015).
17. Hoogewind, K. A., Baldwin, M. E. & Trapp, R. J. The impact of climate change on hazardous convective weather in the United States: Insight from high-resolution dynamical downscaling. *J. Clim.* **30**, 10081–10100 (2017).
18. Liu, C. et al. Continental-scale convection-permitting modeling of the current and future climate of North America. *Clim. Dyn.* **49**, 71–95 (2017).
19. Gensini, V. A., Haberlie, A. M. & Ashley, W. S. Convection-permitting simulations of historical and possible future climate over the contiguous United States. *Clim. Dyn.* **60**, 109–126 (2023).
20. Seneviratne, S. I. et al. Weather and climate extreme events in a changing climate. In *Climate change 2021: the physical science basis. Contribution of Working Group I to the Sixth Assessment Report of the Intergovernmental Panel on Climate Change* (Cambridge University Press, 2021).
21. Haberlie, A. M. & Ashley, W. S. A radar-based climatology of mesoscale convective systems in the United States. *J. Clim.* **32**, 1591–1606 (2019).
22. Trenberth, K. E., Dai, A., Rasmussen, R. M. & Parsons, D. B. The changing character of precipitation. *Bull. Am. Meteorol. Soc.* **84**, 1205–1218 (2003).
23. Trapp, R. J., Hoogewind, K. A. & Lasher-Trapp, S. Future changes in hail occurrence in the United States determined through convection-permitting dynamical downscaling. *J. Clim.* **32**, 5493–5509 (2019).
24. Rasmussen, K. L., Prein, A. F., Rasmussen, R. M., Ikeda, K. & Liu, C. Changes in the convective population and thermodynamic environments in convection-permitting regional climate simulations over the United States. *Clim. Dyn.* **55**, 383–408 (2020).
25. Haberlie, A. M., Ashley, W. S., Battisto, C. M. & Gensini, V. A. Thunderstorm activity under intermediate and extreme climate change scenarios. *Geophys. Res. Lett.* **49**, e2022GL098779 (2022).
26. Ashley, W. S., Haberlie, A. M. & Gensini, V. A. The future of supercells in the United States. *Bull. Am. Meteorol. Soc.* **104**, E1–E21 (2023).
27. Prein, A. F., Rasmussen, R. M., Wang, D. & Giangrande, S. E. Sensitivity of organized convective storms to model grid spacing in current and future climates. *Philos. Trans. R. Soc. A* **379**, 20190546 (2021).
28. Hurrell, J. W. et al. The community earth system model: a framework for collaborative research. *Bull. Am. Meteorol. Soc.* **94**, 1339–1360 (2013).
29. Bruyère, C. L., Done, J. M., Holland, G. J. & Fredrick, S. Bias corrections of global models for regional climate simulations of high-impact weather. *Clim. Dyn.* **43**, 1847–1856 (2014).
30. Creighton, G., et al. AFWA diagnostics in WRF. https://citeseerx.ist.psu.edu/document?repid=rep1&type=pdf&doi=5b4876dc88613a9cf49ec6c33f35317b01c63232 (2014).
31. Haberlie, A. M. & Ashley, W. S. Climatological representation of mesoscale convective systems in a dynamically downscaled climate simulation. *Int. J. Climatol.* **39**, 1144–1153 (2019).
32. Lakshmanan, Miller, V. M. & Smith, T. Quality control of accumulated fields by applying spatial and temporal constraints. *J. Atmos. Ocean. Tech.* **30**, 745–758 (2013).
33. Prein, A. F., Ge, M., Ramos-Valle, A. N., Wang, D. & Giangrande, S. E. Towards a Unified Setup to Simulate Mid-Latitude and Tropical Mesoscale Convective Systems at Kilometer-Scales. *Earth Space Sci.* **9**, e2022EA002295 (2022).
34. Duda, J. D., Wang, X. & Xue, M. Sensitivity of convection-allowing forecasts to land surface model perturbations and implications for ensemble design. *Mon. Weather Rev.* **145**, 2001–2025 (2017).

ACKNOWLEDGEMENTS

The authors would like to acknowledge high-performance computing support from Cheyenne (https://doi.org/10.5065/D6RX99HX) provided by NCAR's Computational and Information Systems Laboratory, sponsored by the National Science Foundation. This research was supported by the National Science Foundation award numbers 1637225, 1800582, and 2203516 and the National Oceanic and Atmospheric Administration award number NA22OAR4690645. The authors also would like to acknowledge and thank Dr. Michael Papka (Argonne) and the Argonne Leadership Computing Facility at Argonne National Laboratory for data storage and post processing assistance. This research used resources of the Argonne Leadership Computing Facility, which is a DOE Office of Science User Facility supported under Contract DE-AC02-06CH11357.

AUTHOR CONTRIBUTIONS

A.H. designed the research approach, carried out the data analysis, and wrote the original paper. W.A. assisted in the research approach design and edited the paper. V.G. and A.M. conducted the numerical experiments, performed initial validation on the numerical modeling output, and edited the paper. All authors contributed to the paper and approved the submitted version.

COMPETING INTERESTS

The authors declare no competing interests.

ADDITIONAL INFORMATION

Supplementary information The online version contains supplementary material available at https://doi.org/10.1038/s41612-023-00481-5.

Correspondence and requests for materials should be addressed to Alex M. Haberlie.

Reprints and permission information is available at http://www.nature.com/reprints

Publisher's note Springer Nature remains neutral with regard to jurisdictional claims in published maps and institutional affiliations.